Wideband Planar Inverted-F MIMO Antenna with High Isolation

Zhaoyang Tang[*]**, Bo Wang, Yingzeng Yin, and Ruina Lian**

Abstract—A wideband planar inverted-F MIMO antenna with high isolation is proposed in this letter. The proposed MIMO antenna consists of two back-to-back planar inverted-F antennas and a fork-shaped decoupling stub. The two planar inverted-F antennas are merged together with a shorting strip connected to the ground plane. In order to enhance the isolation, a fork-shaped decoupling stub connected to the ground plane through shorting pins is introduced, and the impedance matching is significantly improved simultaneously. The proposed antenna prototype is fabricated and measured, and a compact size of $28 \times 26 \, \text{mm}^2$ makes the proposed antenna be easily integrated in a MIMO system. Measured results show that the measured bandwidth for $|S_{11}|$ less than $-10 \, \text{dB}$ covers from $5.05 \, \text{GHz}$ to $6.23 \, \text{GHz}$, and the measured isolation is higher than $20 \, \text{dB}$ in the whole working frequency band.

1. INTRODUCTION

In modern wireless communication applications, multiple-input multiple-out technique regarded as a practical method to implement reliability and extend channel capacity without adding additional power or spectrum has drawn much interest [1]. However, when the antennas are placed closely, strong mutual coupling among antenna elements will degrade the performance of a MIMO system. Thus, improving isolation is desirable in a MIMO system. Furthermore, the antennas must be as compact as possible to be easily integrated in a MIMO system.

In recent years, many methods have been explored to deal with the isolation characteristic of a MIMO system [2–11]. In the design of [2], a folded resonator with about half a guided wavelength placed above the antenna is used to improve the isolation. Compared with the integrated PIFA without the folded resonator, the isolation of the proposed antenna is significantly improved. In [3], a smaller square branch at the opposite ground corner is used to improve high isolation, and the antenna with a measured isolation better than $25 \, \text{dB}$ presents a bandwidth of 12.4%. A T-shaped shorting strip is applied into a three-antenna MIMO system to suppress the mutual coupling [4]. In the design of [5], a shorting strip and an isolation stub are designed to improve isolation. The measured isolation values are better than 25 and $20 \, \text{dB}$ at the $2.45 \, \text{GHz}$ and $5.8 \, \text{GHz}$ bands, respectively. Many slots with different lengths are employed to implement high isolation [6, 7]. In [8], a tree-like structure is proposed to suppress surface wave propagation so as to reduce mutual coupling between radiating elements, and the measured isolation in the whole bandwidth exceeds $16 \, \text{dB}$. In [9], two shorting pins are introduced to reduce the coupling between the feeding ports, and the isolation can be enhanced to more than $40 \, \text{dB}$. High port isolation is implemented by employing anti-phase feeding technique [10, 11]. However, the feed network is relatively complicated, and the radiation performance is affected by the power divider.

In this letter, a wideband planar inverted-F MIMO antenna with high isolation is presented. A common shorting strip connected to the ground plane is used to merge the planar inverted-F antennas together. In order to enhance the isolation, a fork-shaped decoupling stub is introduced via shorting pins connecting to the ground plane. At the same time, the impedance matching is well achieved. The details of the proposed antenna design and measured results are in the following sections.

* Corresponding author: Zhaoyang Tang (zhaoyangt@126.com).

The authors are with the National Key Laboratory of Antennas and Microwave Technology, Xidian University, Xi'an, Shaanxi 710071, People's Republic of China.

2. ANTENNA DESIGN AND DISCUSSION

The geometry and photograph of the proposed antenna is shown in Figure 1. The proposed antenna consists of two back-to-back planar inverted-F antennas and a fork-shaped decoupling stub. The antenna is printed on a low-cost FR4 glass epoxy substrate with a dielectric constant of 4.4 and a loss tangent of 0.02. The planar inverted-F antennas and ground plane in light gray color are printed on the top layer of the substrate, while the fork-shaped decoupling stub in dark gray color is printed on the bottom layer of the substrate. The size of the proposed antenna is $28 \times 26 \times 1\,\mathrm{mm}^3$ ($W \times L \times h$). The standard design formula for a PIFA is:

$$f_0 = \frac{C}{4\left(W_1 + L_2\right)\sqrt{\varepsilon_{\mathit{eff}}}} \tag{1}$$

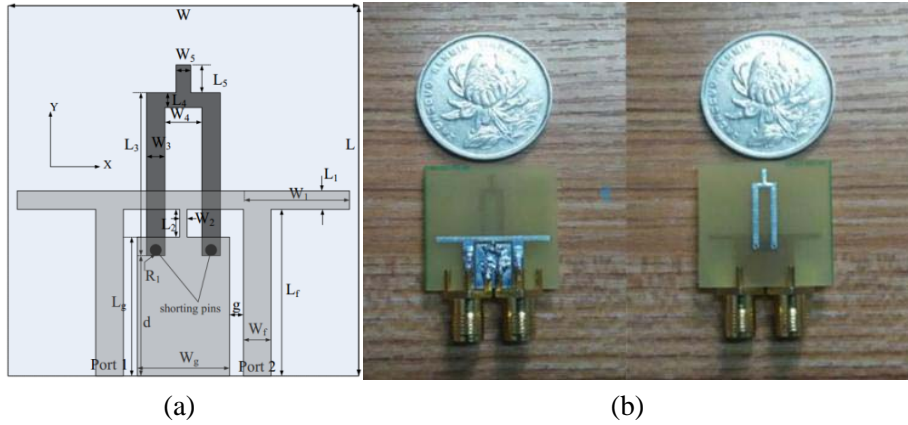(a)   (b)

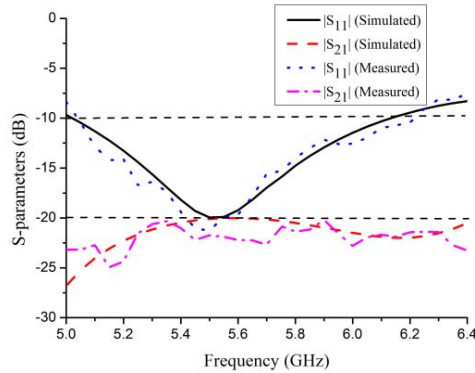**Figure 1.** Geometry and photograph of the proposed antenna. (a) Geometry. (b) Photograph.

Figure 2. S-parameter characteristics of the proposed antenna.

Table 1. Optimized design parameters of the proposed antenna (unit: mm).

L_f	W_f	g	L_1	W_1	L_2	W_2	L_3	W_3
9	2	0.3	1	7.4	1	0.6	10.6	1.3
L_4	W_4	L_5	W_5	L_g	W_g	d	R_1	
1.1	2.6	1.9	1.3	8	6	7.2	0.3	

where f_0 is the resonant frequency of the main mode; c is the speed of light in the free space; ε_{eff} is defined as the effective dielectric constant of structure; W_1 and L_2 are length and height of the radiation element, respectively. To obtain the required numerical analysis and proper geometrical parameters, a three-dimensional EM-simulator (Ansoft HFSS 13.0) is carried out. The optimized design parameters are listed in Table 1.

The Anritsu 37269A vector network analyser is used to measure the bandwidth performance of the proposed antenna. Figure 2 shows the simulated and measured results of the S-parameters of the proposed antenna. It can be seen that the measured bandwidth for $|S_{11}|$ less than -10 dB is from 5.05 GHz to 6.23 GHz, and the measured isolation is better than 20 dB over the whole working frequency band. A good agreement is obtained between the simulated and measured results with a little difference between them due to weld and fabrication tolerance.

Figure 3 shows the simulated $|S_{11}|$ of the proposed antenna with different radiation element lengths W_1. As W_1 increases from 7 to 7.6 mm with an increase of 0.2 mm, the resonant operating frequency moves toward the lower frequency, which shows that the length of the radiation element determines the resonant frequency of the proposed antenna. In a word, changing W_1 appropriately can adjust the needed resonant operating frequency of the proposed antenna.

Figure 4 shows the simulated $|S_{11}|$ of the proposed antenna with different lengths L_2 of the shorting strip. As L_2 decreases, the resonant operating frequency shifts toward the higher frequency because of the height reduction of radiation element. Moreover, the simulated $|S_{11}|$ significantly lifts up as L_2 decreases, which shows the impedance matching becomes worse. In fact, changing the shorting strip length leads to change the distribution capacity and inductance of the proposed antenna to implement the impedance match.

Strong mutual coupling between the antennas will degrade the performance of a MIMO system, which is necessary to be suppressed. In order to reduce mutual coupling, a fork-shaped decoupling stub is introduced in our design. Figure 5 shows the simulated $|S_{21}|$ for different lengths L_3 of the decoupling stub. Note that significant decrease of $|S_{21}|$ is achieved with an increase of L_3, which reveals the mutual coupling between the planar inverted-F antennas is degraded.

Figure 6 shows the simulated $|S_{21}|$ for different distances W_4 between two arms of the fork-shaped decoupling stub. As W_4 increases from 1.8 to 3 mm in increments of 0.4 mm, the simulated $|S_{21}|$ decreases dramatically. As is shown in Figure 7, the distance W_4 between two arms of the decoupling stub also has an effect on the impedance matching. Obviously, the simulated $|S_{11}|$ decreases as W_4 increases, which indicates the impedance matching is improved.

The simulated S-parameter characteristics with and without the decoupling stub are shown in Figure 8. Without a decoupling stub, the MIMO antenna has the isolation of about 10 dB at the working frequency band. When a decoupling stub is added, the simulated isolation characteristic at the working frequency band exceeds 20 dB, which demonstrates the decoupling stub works, and the impedance matching is well improved simultaneously.
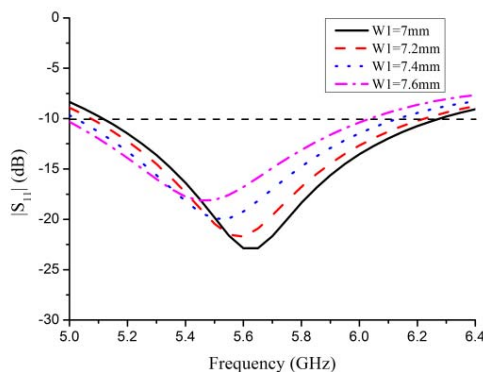

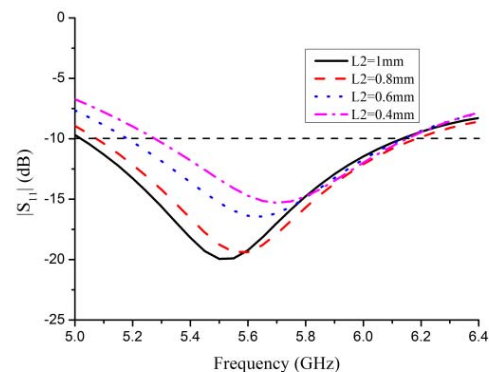**Figure 3.** Simulated $|S_{11}|$ for different W_1.

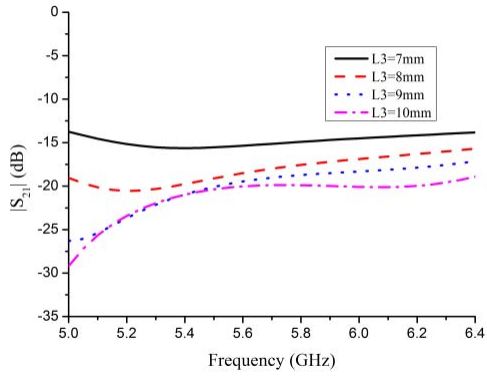**Figure 4.** Simulated $|S_{11}|$ for different L_2.

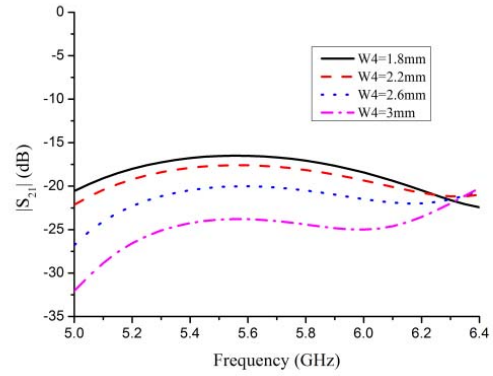**Figure 5.** Simulated $|S_{21}|$ for different L_3.

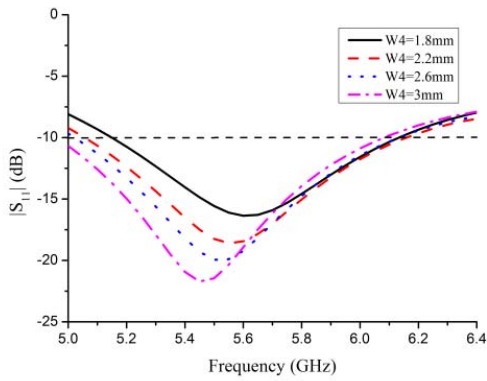**Figure 6.** Simulated $|S_{21}|$ for different W_4.

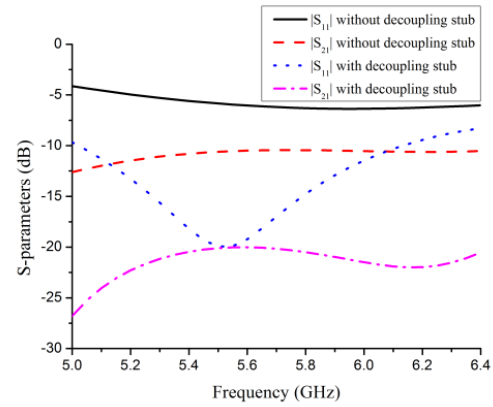**Figure 7.** Simulated $|S_{11}|$ for different W_4.

Figure 8. Simulated S-parameter characteristics with and without the decoupling stub.
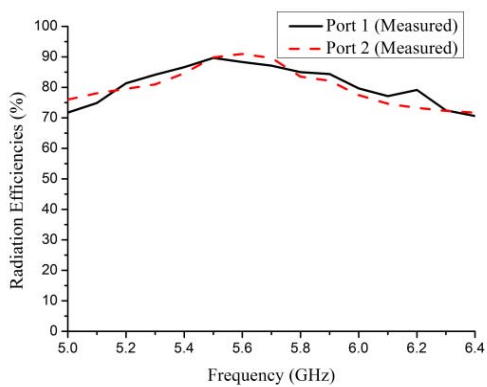

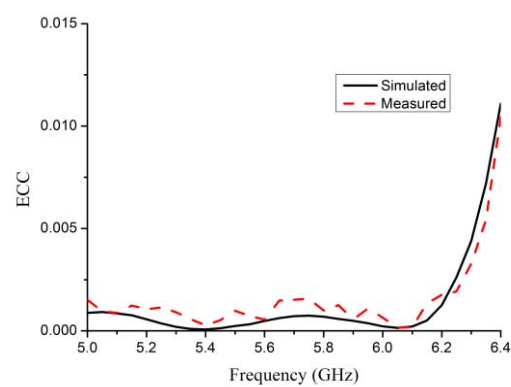**Figure 9.** Measured radiation efficiencies of the proposed antenna.

Figure 10. Simulated and measured ECC.

The measured radiation efficiencies of the antenna with two ports excited are shown in Figure 9. As the figure shows, the radiation efficiencies are above 70% across the measured operating bandwidth. For a MIMO system, the two-port envelope correlation coefficient (ECC) is a critical parameter. The

envelope correlation coefficient (ECC) ρ can be calculated from [12]

$$\rho = \frac{|S_{11}^* S_{12} + S_{21}^* S_{22}|^2}{\left(1 - |S_{11}|^2 - |S_{21}|^2\right)\left(1 - |S_{22}|^2 - |S_{12}|^2\right)} \tag{2}$$

Figure 10 shows the simulated and measured ECC curves based on the simulated and measured data. The measured ECCs are lower than 0.015 in our design. The proposed antenna can lead to good MIMO performance.

Simulated and measured radiation patterns ((a), (b) x-z plane; (c), (d) y-z plane; (e), (f) x-y
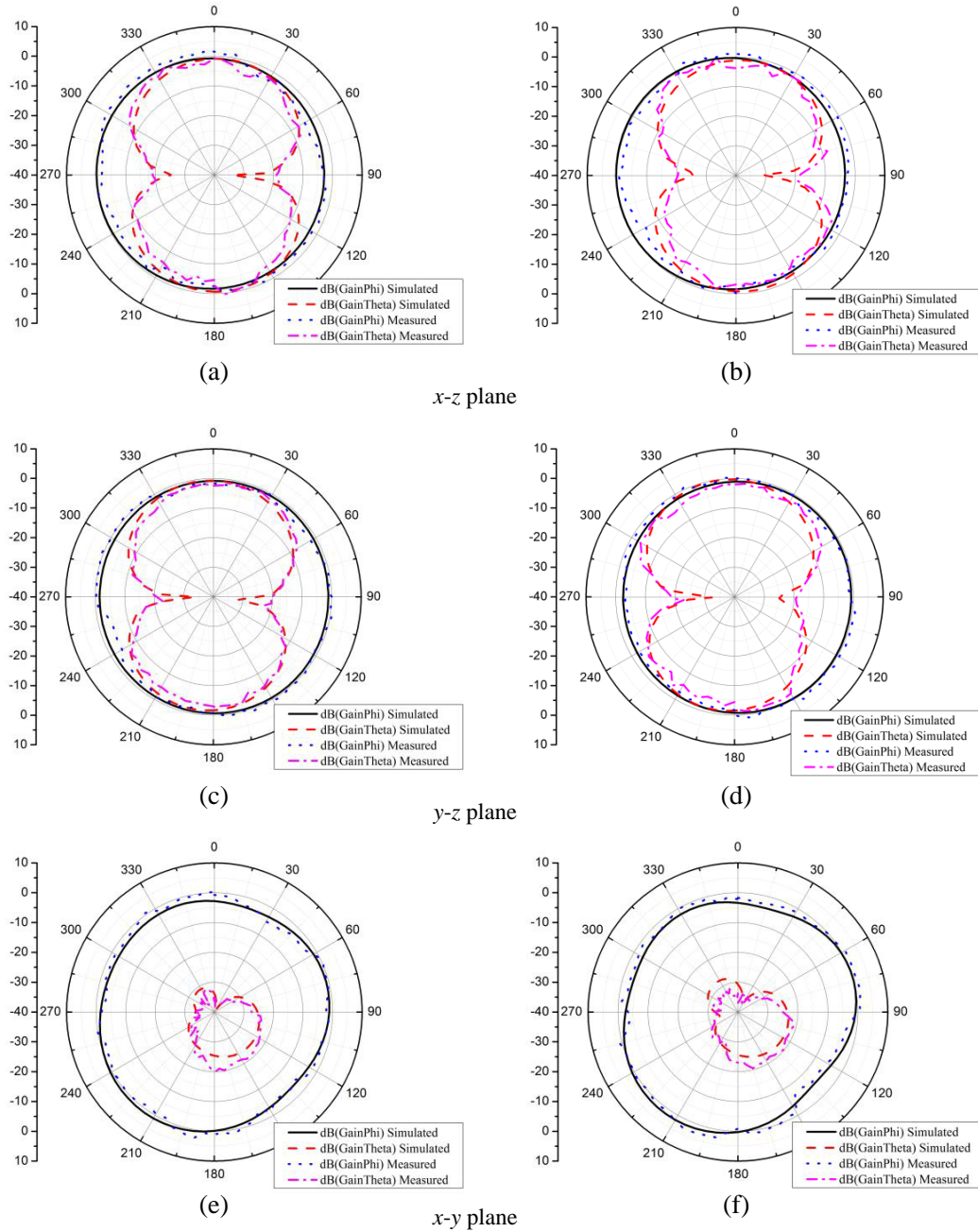

Figure 11. Simulated and measured radiation patterns of the proposed antenna excited from port 1 at (a), (c), (e) 5.2 GHz and (b), (d), (f) 5.8 GHz.

plane) of the proposed antenna excited from port 1 at 5.2 GHz (a), (c), (e) and 5.8 GHz (b), (d), (f) are depicted in Figure 11, while port 2 is terminated by a 50-Ω load. The antenna structure is symmetric about the y-z plane, thus the patterns of the antenna excited from port 2 are similar and symmetric about the y-z plane with those in Figure 11. The measured antenna gains are 1.26 dB at 5.2 GHz and 1.58 dB at 5.8 GHz, respectively.

3. CONCLUSION

In this letter, a wideband planar inverted-F MIMO antenna with high isolation is proposed. A prototype of the proposed antenna is fabricated and measured to demonstrate the effectiveness of the design. A measured operating bandwidth for $|S_{11}|$ less than -10 dB is from 5.05 GHz to 6.23 GHz, and the measured isolation is higher than 20 dB over the working frequency band. The high isolation performance is achieved by introducing a fork-shaped decoupling stub. The simple structure and high isolation make the proposed design suitable for wireless communication applications.

REFERENCES

1. Murch, R. D. and K. B. Letaief, "Antenna systems for broadband wireless access," *IEEE Commun. Mag.*, Vol. 40, No. 4, 76–83, Apr. 2002.
2. Lee, C. H., S. Y. Chen, and P. W. Hsu, "Intergrated dual planar inverted-F antenna with enhanced isolation," *IEEE Antennas Wireless Propag. Lett.*, Vol. 8, 963–965, 2009.
3. Lai, X. Z., Z. M. Xie, X. L. Cen, and Z. Y. Zheng, "A novel technique for broadband circular polarized PIFA and diversity PIFA systems," *Progress In Electromagnetics Research*, Vol. 142, 41–55, 2013.
4. Wong, K. L., C. H. Chang, B. Chen, and S. Yang, "Three-antenna MIMO system for WLAN operation in a PDA phone," *Microw. Opt. Technol. Lett.*, Vol. 48, 1238–1242, 2006.
5. Ling, X. M. and R. L. Li, "A novel dual-band MIMO antenna array with low mutual coupling for portable wireless devices," *IEEE Antennas Wireless Propag. Lett.*, Vol. 10, 1039–1042, 2011.
6. Sonkki, M. and E. Salonen, "Low mutual coupling between monopole antennas by using two $\lambda/2$ slots," *IEEE Antennas Wireless Propag. Lett.*, Vol. 9, 138–141, 2010.
7. Chiu, C. Y., C. H. Cheng, R. D. Murch, and C. R. Rowell, "Reduction of mutual coupling between closely-packed antenna elements," *IEEE Trans. Antennas Propag.*, Vol. 55, No. 6, 1732–1738, Jun. 2007.
8. Zhang, S., Z. Ying, J. Xiong, and S. He, "Ultrawideband MIMO/diversity antennas with a tree-like structure to enhance wideband isolation," *IEEE Antennas Wireless Propag. Lett.*, Vol. 8, 1279–1282, 2009.
9. Xie, J. J., Y. Z. Yin, J. H. Wang, and X. L. Liu, "Wideband dual-polarised electromagnetic-fed patch antenna with high isolation and low cross-polarisation," *Electron. Lett.*, Vol. 49, No. 3, 171–173, 2013.
10. Wong, K. L. and T. W. Chiou, "Broad-band dual-polarized patch antennas fed by capacitively coupled feed and slot-coupled feed," *IEEE Trans. Antennas Propag.*, Vol. 50, No. 3, 346–351, Mar. 2002.
11. Chiou, T. W. and K. L. Wong, "Broad-band dual-polarized single microstrip patch antenna with high isolation and low cross polarization," *IEEE Trans. Antennas Propag.*, Vol. 50, No. 3, 399–401, Mar. 2002.
12. Blanch, S., J. Romeu, and I. Corbella, "Exact representation of antenna system diversity performance from input parameter description," *Electron. Lett.*, Vol. 39, No. 9, 705–707, May 2003.